ELSEVIER

Journal of Structural Geology 28 (2006) 1685–1693

JOURNAL OF STRUCTURAL GEOLOGY

www.elsevier.com/locate/jsg

Displacement accumulation from earthquakes on isolated normal faults

T. Manzocchi [a,*], J.J. Walsh [a], A. Nicol [a,b]

[a] Fault Analysis Group, School of Geological Sciences, University College Dublin, Belfield, Dublin 4, Ireland
[b] GNS Science, Lower Hutt, New Zealand

Received 26 October 2005; received in revised form 8 June 2006; accepted 20 June 2006
Available online 21 August 2006

Abstract

Displacement profiles for isolated normal faults are most often triangular rather than semi-elliptical as predicted for linear elastic materials. Simple modelling indicates that triangular displacement profiles can arise from Gutenberg–Richter earthquakes randomly distributed on fault surfaces of constant dimensions. Near-triangular profiles are generated after a small number of earthquake cycles and for earthquake magnitude ranges as small as 0.5. The results are only weakly dependent on the shape of earthquake slip profiles, and reproduce the geometry of displacement profiles on the non-propagating active Cape Egmont Fault in New Zealand. By contrast, growth models in which fault displacement and length increase in proportion result in unrealistic displacement profiles for realistic slip profiles irrespective of whether earthquake populations are Characteristic or Gutenberg–Richter.

Keywords: Faults; Fault growth; Fault displacement; Characteristic earthquakes; Gutenberg–Richter

1. Introduction

Earthquake slip events are ideally characterised by the semi-elliptical slip profiles expected for ruptures within linear elastic materials (Eshelby, 1957; Pollard and Segall, 1987). It is now generally accepted, however, that these slip profiles combine to provide long-term displacement profiles that are most often triangular in shape, with departures from triangular displacement profiles generally attributed to strong interactions with adjacent faults or to rheological effects (Nicol et al., 1996; Manighetti et al., 2001). A variety of fault growth models have been advanced to explain both the triangular shape of displacement profiles and the well-established displacement/length scaling on faults (Walsh and Watterson, 1987; Cowie and Scholz, 1992; Manighetti et al., 2004). A feature of all such models is that each slip event ruptures the entire fault surface, providing Characteristic earthquakes (Schwartz and Coppersmith, 1984), and is responsible for fault propagation. The predicted propagation is independent of whether elastic strains are relaxed between each slip increment (Walsh and Watterson, 1987), permitted to accrue on the fault (Cowie and Scholz, 1992) or partially relieved by minor faulting in a damage zone (Manighetti et al., 2004). A growing body of evidence suggests, however, that fault propagation is a feature principally of the earliest phase of fault activity and that normal faults often accumulate displacement whilst maintaining near constant lengths for the majority of their growth history (Morewood and Roberts, 1999; Poulimenos, 2000; Meyer et al., 2002; Walsh et al., 2002; Childs et al., 2003; Nicol et al., 2005). In these circumstances, triangular profiles can only be produced by relaxing the requirements for Characteristic earthquakes or by abandoning the notion of semi-elliptical slip profiles.

In this paper we reproduce the triangular displacement profiles that are typical of non-interacting faults using a simple stochastic model in which a Gutenberg–Richter (G–R) (i.e. power-law; Gutenberg and Richter, 1944) population of earthquakes occurs on a fault surface of fixed dimensions. The placement of earthquakes on the fault is assumed to be entirely random on the basis that (i) associated elastic strains are

* Corresponding author. Tel.: +353 1 7162605; fax: +353 1 7162607.
E-mail address: tom@fag.ucd.ie (T. Manzocchi).

0191-8141/$ - see front matter © 2006 Elsevier Ltd. All rights reserved.
doi:10.1016/j.jsg.2006.06.006

relaxed on geological time scales (e.g. thousands to millions of years) and (ii) the spatio-temporal correlations of earthquake behaviour on isolated faults is a short-term phenomenon, occurring on time scales much less than the several G–R cycles examined in our modelling. Results indicate that even after small numbers of earthquake cycles and very modest (>0.5) ranges in earthquake magnitude, near-triangular profiles are generated irrespective of the shape of earthquake slip profiles.

A comparison of model results with the Cape Egmont Fault from New Zealand's Taranaki Basin, which did not grow in length during much of its most recent period of growth (0–3.7 Ma BP) indicates that it is not possible to infer either the shapes of slip events or the magnitude range of earthquakes from the shape of the displacement profiles – the near-triangular displacement profiles observed on nine horizons could have arisen from a variety of earthquake slip profiles, including elliptical ones, and for different ranges in earthquake magnitudes.

Finally, we re-examine existing inelastic geometrical fault profile evolution models for propagating faults (e.g. Walsh and Watterson, 1988; Gillespie et al., 1992; Peacock and Sanderson, 1996) and include G–R, as well as Characteristic, earthquake populations in the models. Results indicate that elliptical slip distributions can generate near-triangular displacement distributions on propagating faults only if the earthquake population is near-Characteristic and if the displacement/length scaling exponent is higher than generally measured ($n > 1.5$).

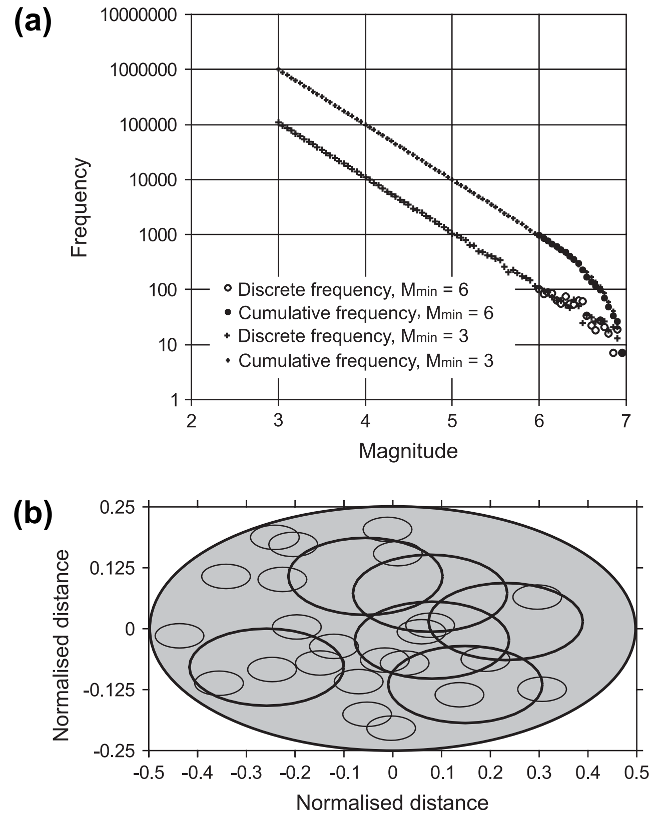

Fig. 1. (a) Magnitude frequency and cumulative frequency of earthquake populations for realisations of 100 G–R cycles covering earthquake magnitude ranges of 4 and 1. (b) Idealised elliptical model fault (grey) showing the rupture areas of six M6 and 20 M5 randomly positioned earthquakes.

2. Displacement profiles for non-propagating faults

A stochastic model of a G–R population of earthquakes is used to simulate normal fault growth by the accumulation of co-seismic slip (Fig. 1). For illustrative purposes, we have chosen to model an elliptical fault surface capable of supporting a maximum earthquake of magnitude 7. G–R populations containing earthquakes of magnitude $7 > M \geq M_{\min}$ are generated for different values of $M_{\min}$ and a range of G–R cycles. Each population defines a power-law magnitude frequency distribution over the modelled range in M, while the cumulative magnitude frequency distribution shows the characteristic roll-off (e.g. Main, 1990) at high M (Fig. 1a). The value of the cumulative frequency population extrapolated to M7 is equivalent to the number of G–R cycles present. Models considered contain up to 10^7 earthquakes, between 0.1 and 100 G–R cycles and with $M_{\min}$ ranging from 2 to 6.9.

The moment (M_0) of an earthquake is related empirically to its magnitude through $\log(M_0) = cM + d$, where $c \approx 1.5$ and $d \approx 9.1$ (e.g. Scholz, 1990), and to the dimensions of the rupture through $M_0 = \mu \langle u \rangle A$, where μ is the shear modulus (taken as 10 GPA, e.g. Walsh and Watterson, 1988), $\langle u \rangle$ is the average co-seismic slip and A is the rupture area. We model elliptical ruptures with principal radii of length $r_1 = 2r_2$ (Fig. 1b). The empirical ratio between maximum co-seismic slip ($u_{\max}$) and rupture length ($2r_1$) of 5×10^{-5} (Wells and Coppersmith, 1994) is used. Each model comprises earthquake ruptures with one of three slip shapes: conical profiles (triangular in 1D) in which $\langle u \rangle = u_{\max}/3$, semi-ellipsoidal profiles (elliptical in 1D) in which $\langle u \rangle = 2u_{\max}/3$, and disc-shaped profiles (rectangular in 1D) in which $\langle u \rangle = u_{\max}$ (Fig. 2). These relationships define the dimensions ($u_{\max}$, r_1) of each model earthquake from its magnitude. For example, a conical M7 model earthquake has a maximum slip of 4.2 m and a maximum rupture length of 85 km, while a disc-shaped one has $u_{\max} = 2.9$ m and $2r_1 = 59$ km. The smallest events considered (M2) have $u_{\max} \approx 1$ cm and $2r_1 \approx 200$ m. The fault surface is scaled by the dimensions of the largest possible earthquake (M7) and individual ruptures are placed randomly on the fault with the single constraint that each rupture must be contained entirely within the fault surface (Fig. 1b).

Models with elliptical slip profiles, $M_{\min} = 4$ and different numbers of G–R cycles are discussed (Figs. 3 and 4) before examining the dependence of the shape of the slip profiles and the range of earthquake sizes on the resultant displacement profiles (Fig. 5). The accumulation of displacement is examined either on the entire fault surface (e.g. Fig. 3a–c) or on 1D sections through the long axis of the fault (Fig. 3d–f). Profiles on any other chord of the fault are broadly similar in shape. Profiles at fractions of a G–R cycle are characterised by high displacement gradients and irregular shapes (Fig. 3a) but as the fault accumulates more earthquakes the shape of the profile becomes gradually more regular (Fig. 3b). An essentially smooth displacement profile emerges